INTERFACE FOCUS

royalsocietypublishing.org/journal/rsfs

Research

Cite this article: Jeong EM, Song YM, Kim JK. 2022 Combined multiple transcriptional repression mechanisms generate ultrasensitivity and oscillations. *Interface Focus* **12**: 20210084.
https://doi.org/10.1098/rsfs.2021.0084

Received: 10 November 2021
Accepted: 24 February 2022

One contribution of 5 to a theme issue 'Time-keeping and decision-making in living cells; Oscillations and Synchronization (Part I)'.

Subject Areas:
systems biology, computational biology, biomathematics

Keywords:
transcriptional repression, sequestration, displacement, ultrasensitivity, biological oscillators, circadian clock

Author for correspondence:
Jae Kyoung Kim
e-mail: jaekkim@kaist.ac.kr

Electronic supplementary material is available online at https://doi.org/10.6084/m9.figshare.c.5880153.

THE ROYAL SOCIETY PUBLISHING

Combined multiple transcriptional repression mechanisms generate ultrasensitivity and oscillations

Eui Min Jeong[1,2], Yun Min Song[1,2] and Jae Kyoung Kim[1,2]

[1]Department of Mathematical Sciences, Korea Advanced Institute of Science and Technology, Daejeon 34141, Republic of Korea
[2]Biomedical Mathematics Group, Institute for Basic Science, Daejeon 34126, Republic of Korea

JKK, 0000-0001-7842-2172

Transcriptional repression can occur via various mechanisms, such as blocking, sequestration and displacement. For instance, the repressors can hold the activators to prevent binding with DNA or can bind to the DNA-bound activators to block their transcriptional activity. Although the transcription can be completely suppressed with a single mechanism, multiple repression mechanisms are used together to inhibit transcriptional activators in many systems, such as circadian clocks and NF-κB oscillators. This raises the question of what advantages arise if seemingly redundant repression mechanisms are combined. Here, by deriving equations describing the multiple repression mechanisms, we find that their combination can synergistically generate a sharply ultrasensitive transcription response and thus strong oscillations. This rationalizes why the multiple repression mechanisms are used together in various biological oscillators. The critical role of such combined transcriptional repression for strong oscillations is further supported by our analysis of formerly identified mutations disrupting the transcriptional repression of the mammalian circadian clock. The hitherto unrecognized source of the ultrasensitivity, the combined transcriptional repressions, can lead to robust synthetic oscillators with a previously unachievable simple design.

1. Introduction

Transcription, the first step of gene expression, is regulated by activators and repressors, i.e. the bindings of the activators and repressors to a specific DNA sequence promote and downregulate transcription, respectively [1,2]. The repressors can also indirectly inhibit transcription by binding with the activators rather than with DNA (figure 1*a*) [3,4]. That is, the repressors can bind to the DNA-bound activators to block their transcriptional activity (blocking; figure 1*a*), hold the activators to prevent them from binding with DNA (sequestration; figure 1*a*), and dissociate the activators from DNA by forming a complex (displacement; figure 1*a*).

Each repression mechanism appears to be able to suppress transcription solely. However, various repressors use a combination of multiple repression mechanisms [3]. For example, retinoblastoma (Rb) protein, a key regulator of mammalian cell cycle genes, represses transcription by blocking the activator and recruiting histone deacetylase, which alters the structure of chromatin [5–7]. Similarly, PHO80, a component of a yeast nutrient-responsive signalling pathway, represses transcription by blocking the activator and sequestering the activator in the cytoplasm [8–10]. This raises the question of the advantages of using a combination of multiple repression mechanisms, which seems redundant.

In the transcriptional negative feedback loop (NFL) of various biological oscillators, repressors also inhibit their own transcriptions via combinations of the multiple repression mechanisms. For example, IκBα inhibits its own

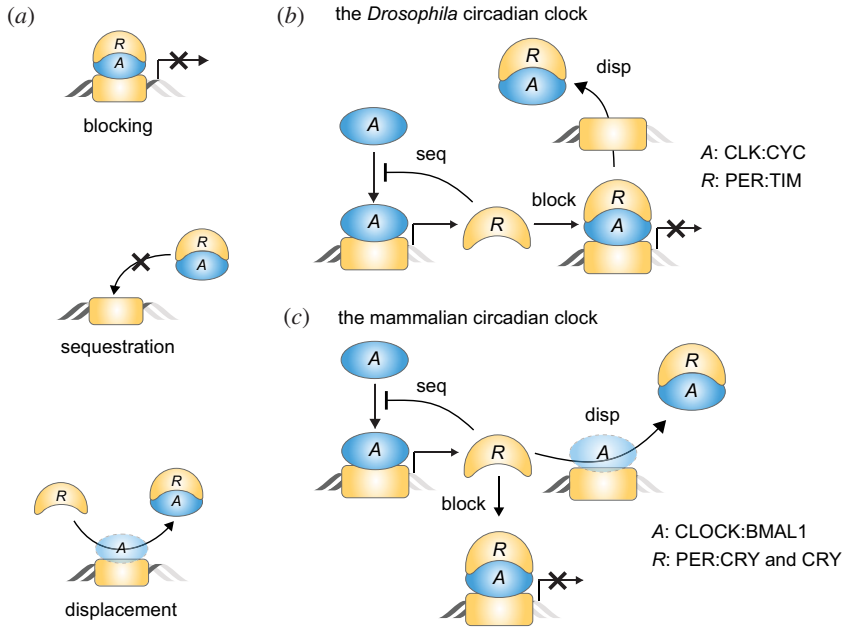

Figure 1. Multiple transcriptional repression mechanisms are used together in the transcriptional NFL of the circadian clock. (*a*) Repressors (*R*) can suppress the transcriptional activity of activators (*A*) with multiple mechanisms. For example, *R* binds to the DNA-bound *A* to block its transcriptional activity (blocking), holds *A* to prevent binding to DNA (sequestration), or dissociates *A* from DNA (displacement). (*b*) Such multiple repression mechanisms are used together in the transcriptional NFL of the *Drosophila* circadian clock. The activator CLK:CYC (*A*) promotes the synthesis of the repressor PER:TIM (*R*). Then, *R* inhibits the transcriptional activity of *A* in various ways: *R* sequesters the free *A* from DNA, and blocks the transcriptional activity of the DNA-bound *A* and then displaces it from DNA. (*c*) Similarly, in the mammalian circadian clock, the repressors PER:CRY and CRY (*R*) inhibit their own transcriptional activator CLOCK:BMAL1 (*A*) via blocking, sequestration and displacement.

transcriptional activator NF-κB by sequestering it in the cytoplasm [11] as well as displacing it from DNA [12,13], which induces the NF-κB oscillation under stress conditions. In the transcriptional NFL of the circadian clock, the transcription is also suppressed in multiple ways. Specifically, in the *Drosophila* circadian clock, the repressor (PER : TIM) sequesters its own transcriptional activator (CLK:CYC) from DNA (sequestration), blocks the transcriptional activity by binding to DNA-bound CLK:CYC (blocking), and then displaces it from DNA (displacement; figure 1*b*) [14]. Similarly, in the mammalian circadian clock, the repressors (PER:CRY and CRY) also inhibit their own transcriptional activator (CLOCK:BMAL1) by sequestration, blocking and displacement (figure 1*c*) [15–17].

The transcriptional NFL can generate oscillations when the transcriptional activity shows an ultrasensitive response to changes in the concentration of repressors [18–21]. Such ultrasensitivity can be generated solely by sequestration when the activators and repressors tightly bind [22,23]. In particular, the sequestration requires only tight binding, which seems to be physiologically more achievable than the conditions for the other ultrasensitivity-generating mechanisms based on cooperativity (e.g. cooperative oligomerization). Thus, sequestration has recently been adopted for mathematical models of circadian clocks [21,24–31]. However, Heidebrecht *et al.* pointed out that the tightness of the binding between the activator and repressor required for the sequestration to generate sustained rhythms is beyond the physiologically plausible binding affinity [32].

Here, we find that combining multiple transcriptional repression mechanisms can synergistically generate ultrasensitivity by deriving their governing equations. Specifically, we find that the sole blocking-type repression can generate only low-sensitivity transcriptional activity. When sequestration is added, the ultrasensitivity can be generated with stronger sequestration compared to the blocking. The required strong sequestration is challenging to achieve with a physiologically plausible binding affinity. Interestingly, this limitation to generate ultrasensitivity and strong oscillations can be overcome by adding displacement. To test whether the combination of the multiple repressions is critical for the mammalian circadian clock to generate strong rhythms, we investigated the previously identified mutations disrupting the transcriptional repressions [33–36]. Indeed, when any of the blocking, sequestration or displacement was disrupted, the circadian rhythms of PER2-LUC became weaker in mice. Our work explains why the combination of seemingly redundant repression mechanisms is used in various systems requiring ultrasensitivity, such as the cell cycle and the circadian clock.

2. Results

2.1. The sole blocking-type repression generates a hyperbolic response in the transcriptional activity

To investigate how the transcription is regulated by the multiple repression mechanisms (figure 1*a*), we first constructed a model describing the single blocking-type repression (figure 2*a*; see Methods for details). In the model, the transcription is triggered when the free activator (A) binds to the free DNA (E_F) with a dissociation constant of K_a to form the activated DNA (E_A). The transcription is inhibited when the repressor (R) binds to the DNA-bound A (E_A) to form ternary complex (E_R) with a dissociation constant of K_b (i.e. the blocking-type repression). Therefore, the transcriptional activity is proportional to the probability that DNA is bound with only A and not R, i.e. E_A/E_T, where $E_T = E_F + E_A + E_R$ is the conserved total concentration of DNA. In particular, when the transcription rate is normalized

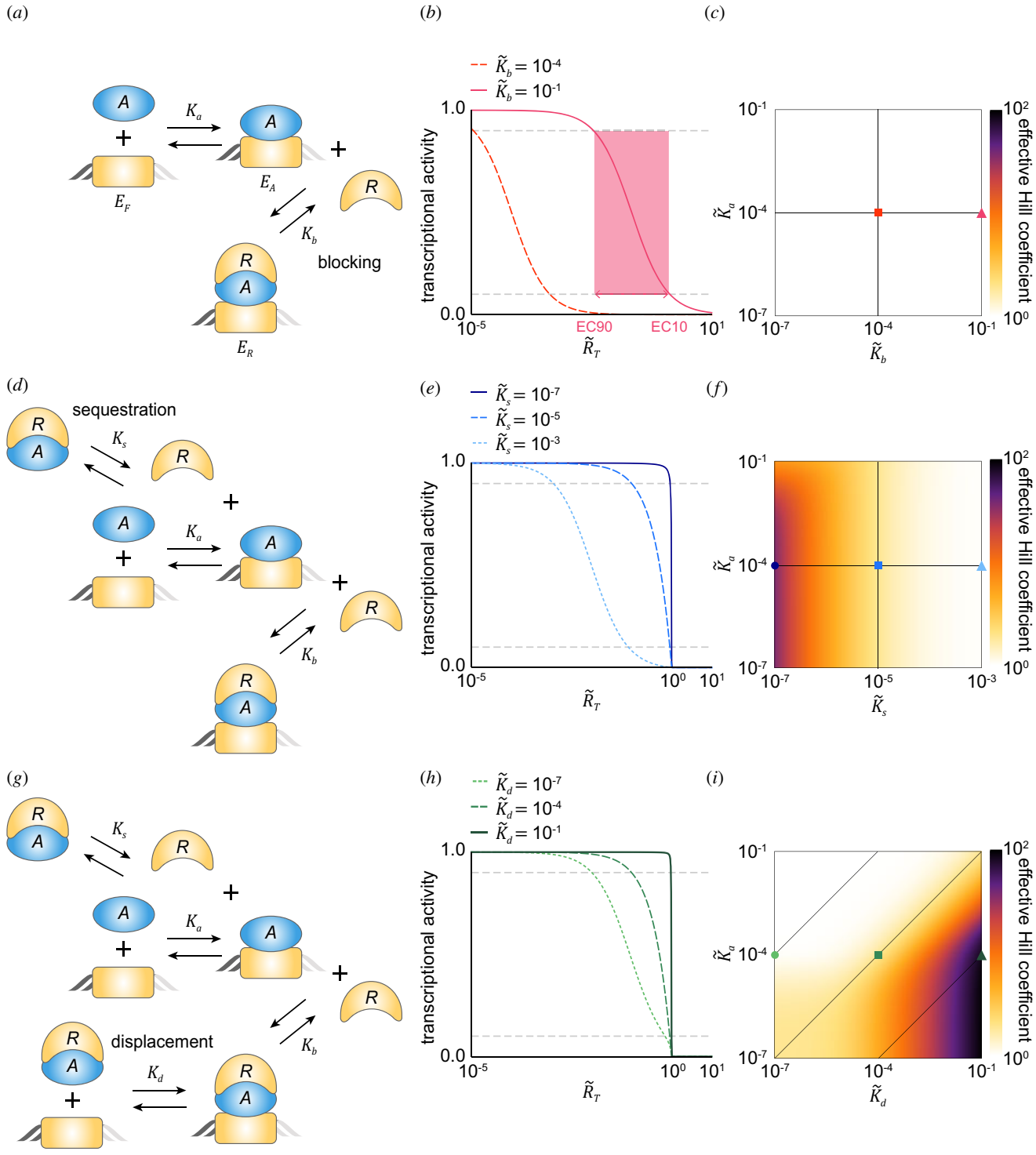

Figure 2. The combination of multiple repression mechanisms leads to ultrasensitive transcription response. (*a*) Diagram of the model describing the blocking-type repression. The binding of the activator (*A*) to DNA with a dissociation constant of K_a leads to the transcription, and the binding of the repressor (*R*) to the DNA-bound *A* with a dissociation constant of K_b, inhibits the transcription. (*b*) As the molar ratio between the total repressor and activator concentrations ($\tilde{R}_T$) increases or their binding affinity increases (i.e. $\tilde{K}_b$ decreases), the transcriptional activity decreases. The sensitivity of the transcriptional activity is quantified using the effective Hill coefficient (Log(81)/Log(EC10/EC90)), which increases as the width of the EC90 and EC10 box decreases (i.e. the red box). The grey dashed lines denote the 10% and 90% values of the maximal transcriptional activity, respectively. Here, $\tilde{K}_a = 10^{-4}$. (*c*) The effective Hill coefficient is one regardless of the values of $\tilde{K}_b$ and $\tilde{K}_a$, indicating that the sole blocking can generate only low sensitivity. The square and triangle marks represent the parameter values used for (*b*). (*d*) The sequestration-type repression is added to the blocking model in (*a*): *R* sequesters the free A with a dissociation constant of K_s from DNA. (*e*) When the sequestration is weaker than the blocking (i.e. $\tilde{K}_s > \tilde{K}_b$; dotted line), the sensitivity of the transcriptional activity is similar to that regulated by only the blocking-type repression (*b*). On the other hand, when the sequestration is stronger than the blocking (i.e. $\tilde{K}_s < \tilde{K}_b$; solid and dashed lines), a switch-like transition in the transcriptional activity occurs. Here, $\tilde{K}_b = 10^{-5}$ and $\tilde{K}_a = 10^{-4}$. (*f*) The effective Hill coefficient increases as $\tilde{K}_s$ decreases. The circle, square and triangle marks represent the parameter values used for (*e*). (*g*) The displacement-type repression is added to the model in (*d*): the R_A complex dissociates from DNA with a dissociation constant of K_d. (*h*) When $\tilde{K}_d = \tilde{K}_a = 10^{-4}$ (dashed line), it satisfies the detailed balance condition (i.e. $\tilde{K}_s\tilde{K}_d/\tilde{K}_b\tilde{K}_a = 1$) and thus the displacement has no effect on the transcriptional activity (cf. dashed line in (*e*)). When the effective displacement occurs (i.e. $\tilde{K}_d > \tilde{K}_a$; solid line), the sensitivity increases. Here, $\tilde{K}_s = 10^{-5}$, $\tilde{K}_b = 10^{-5}$ and $\tilde{K}_a = 10^{-4}$. (*i*) When $\tilde{K}_d > \tilde{K}_a$, the effective Hill coefficients become larger compared to those obtained with the sequestration and blocking (*f*). The circle, square and triangle marks represent the parameter values used for (*h*).

to one, the transcriptional activity and E_A/E_T become the same. Thus, for simplicity, we refer to E_A/E_T as the transcriptional activity throughout this study.

The transcriptional activity (E_A/E_T) increases as A increases or R decreases. This relationship can be quantified by deriving the steady state of E_A/E_T. Because the steady state of E_F depends on the single pair of binding and unbinding reactions with the dissociation constant of K_a, its steady state equation is $AE_F = K_aE_A$. Similarly, the steady state equation of E_R is also simple as $RE_A = K_bE_R$. Therefore, E_F: E_A: $E_R = 1$: A/K_a: $(R/K_b)(A/K_a)$ at the steady state, leading to the steady state of E_A/E_T as follows:

$$\frac{E_A}{E_T} = \frac{A/K_a}{1 + (A/K_a) + (R/K_b)(A/K_a)}, \tag{2.1}$$

where A and R are the steady states of the free activator and repressor, respectively (see Methods for details). Because the steady states of A and R depend on the dissociation constants (i.e. K_a and K_b), it is challenging to analyse equation (2.1).

Equation (2.1) can be further simplified because the concentration of DNA is typically negligible compared to the concentration of activator and repressor proteins (see Methods for details about the validity of the assumption). Specifically, E_A and E_R can be neglected in the conserved total concentration of the activator ($A_T = A + E_A + E_R$) and the repressor ($R_T = R + E_R$), and thus $A \approx A_T$ and $R \approx R_T$. This allows us to get the simplified approximation for equation (2.1) as follows:

$$\frac{E_A}{E_T} \approx \frac{(A_T/K_a)}{1 + (A_T/K_a) + (R_T/K_b)(A_T/K_a)} = \frac{\tilde{K}_b}{\tilde{R}_T + \tilde{K}_b(1 + \tilde{K}_a)}, \tag{2.2}$$

where $\tilde{R}_T = R_T/A_T$ is the molar ratio between R_T and A_T, and $\tilde{K}_b = K_b/A_T$ and $\tilde{K}_a = K_a/A_T$ are the dissociation constants normalized by the concentration of the total activator. Equation (2.2) indicates that the transcriptional activity shows a hyperbolic response with respect to the molar ratio $\tilde{R}_T$ (figure 2*b*). Specifically, when $\tilde{R}_T = 0$, E_A/E_T has the maximum value $1/(1 + \tilde{K}_a)$, which becomes closer to one as A binds to DNA more tightly (i.e. $\tilde{K}_a \ll 1$). When $\tilde{R}_T = \tilde{K}_b(1 + \tilde{K}_a)$, E_A/E_T is reduced to its half-maximal value. Thus, as the binding between the DNA-bound A and R becomes tighter (i.e. $\tilde{K}_b$ decreases), the transcriptional activity achieves its half-maximal value at the lower $\tilde{R}_T$ (figure 2*b*). The sensitivity of the transcriptional activity with respect to $\tilde{R}_T$ can be quantified using the effective Hill coefficient $\mathrm{Log}(81)/\mathrm{Log}(EC10/EC90)$, which is equivalent to the Hill exponent for a Hill curve [37]. The effective Hill coefficient of the transcriptional activity is one regardless of the $\tilde{K}_b$ and $\tilde{K}_a$ values (figure 2*c*), as expected from the Michaelis–Menten-type equation (equation (2.2)). Taken together, with the sole blocking repression, the transcriptional activity cannot sensitively respond to $\tilde{R}_T$.

2.2. The combination of the sequestration- and blocking-type repressions can generate ultrasensitivity

We wondered whether the sensitivity of the transcriptional activity can be increased by incorporating an additional repression mechanism. To investigate this, we added the sequestration-type repression to the blocking model: R binds with the free A to form complex R_A with a dissociation constant of K_s, and thus sequesters A from DNA (figure 2*d*; see Methods for details). Due to the complex R_A, the conservations are switched to $A_T = A + R_A + E_A + E_R$ and $R_T = R + R_A + E_R$. When the binding between A and R is weak (i.e. $\tilde{K}_s = K_s/A_T \gg 1$) and thus R_A is negligible, the steady states of A and R can be approximated with simple A_T and R_T. On the other hand, when the binding is not weak, R_A is not negligible and thus the approximations for the steady states of A and R become slightly complex (see Methods for details):

$$A \approx \frac{A_T - R_T - K_s + \sqrt{(A_T - R_T - K_s)^2 + 4A_TK_s}}{2}, \quad R \approx R_T - (A_T - A). \tag{2.3}$$

When the binding between A and R is extremely tight ($\tilde{K}_s \approx 0$), A and R can be approximated by the simple functions $\max(A_T - R_T, 0)$ and $\max(R_T - A_T, 0)$, respectively [21,28,30]. By substituting equation (2.3) for equation (2.1), the approximated E_A/E_T can be derived:

$$\frac{E_A}{E_T} \approx \frac{\tilde{A}/\tilde{K}_a}{1 + (\tilde{A}/\tilde{K}_a) + (\tilde{R}/\tilde{K}_b)(\tilde{A}/\tilde{K}_a)}, \tag{2.4}$$

where $\tilde{X} = X/A_T$ ($X \in \{A, R, K_a, K_b, K_s\}$). Because $\tilde{A}$ and $\tilde{R}$ are determined by the molar ratio ($\tilde{R}_T = R_T/A_T$), E_A/E_T is still the function of $\tilde{R}_T$ like in equation (2.2).

The transcriptional activity described by equation (2.4) shows more sensitive responses with respect to $\tilde{R}_T$ compared to the blocking model as the sequestration becomes stronger (i.e. $\tilde{K}_s$ decreases; figure 2*e*). Specifically, when the sequestration is weaker than the blocking (i.e. $\tilde{K}_s > \tilde{K}_b$), the transcriptional regulation is mainly governed by the blocking, and thus the transcriptional activity shows a hyperbolic response (figure 2*e*, dotted line) similar to the sole blocking-type repression (figure 2*b*). On the other hand, when the sequestration is stronger than the blocking (i.e. $\tilde{K}_s < \tilde{K}_b$; figure 2*e*, solid line), R is more likely to bind with the free A rather than the DNA-bound A. Thus, when there are more activators than repressors (i.e. $\tilde{R}_T < 1$), the majority of R is bound to the free A, not the DNA-bound A, and thus the high level of transcriptional activity is maintained. As $\tilde{R}_T$ is greater than one and thus the free R, not sequestered by the free A, is available, R can block the DNA-bound A, leading to the rapid drop in the transcriptional activity (figure 2*e*, solid line). This switch-like transition in the transcriptional activity generates the ultrasensitivity (figure 2*e*). Consistently, the effective Hill coefficient increases as the sequestration becomes stronger (i.e. $\tilde{K}_s$ decreases; figure 2*f*).

The ultrasensitivity can be generated when the blocking and sequestration act synergistically (electronic supplementary material, figure S1). That is, when the blocking is stronger than the sequestration ($\tilde{K}_b < \tilde{K}_s$; electronic supplementary material, figure S1a–c), the ultrasensitivity cannot be generated, similar to the sole blocking model (figure 2*c*). When the blocking is too weak ($\tilde{K}_s \ll \tilde{K}_b$), and thus the transcriptional regulation is mainly governed by the sequestration, the DNA-bound activator cannot be

inhibited effectively via blocking. As a result, ultrasensitivity cannot be generated when the activator binds to DNA more tightly than the repressor ($\tilde{K}_a < \tilde{K}_s$; electronic supplementary material, figure S1d,e). Taken together, to generate ultrasensitivity, the appropriate level of blocking and stronger sequestration compared to the blocking are needed. This requires a mechanism for the repressor to have different binding affinities with the free activator and the DNA-bound activator. Furthermore, due to the requirement of stronger sequestration compared to the blocking, the condition is challenging to achieve with physiologically plausible binding affinities. Specifically, the concentration of transcriptional factors (A_T) is 2×10^{-9}–10^{-7} M as their number is 10^4–10^5 (i.e. 2×10^{-20}–10^{-19} mol) and the typical mammalian cell volume is 10^{-11}–10^{-12} l [32,38,39]. Thus, even the extremely high affinity protein whose dissociation constant is picomolar (i.e. $K_s \approx 10^{-12}$ M) has $\tilde{K}_s$ with the range of 0.5×10^{-5}–10^{-3}. With these physiologically plausible values of $\tilde{K}_s$, the range of $\tilde{K}_b$ where the ultrasensitivity can be generated is narrow (electronic supplementary material, figure S1).

2.3. The combination of the displacement-, sequestration- and blocking-type repressions can readily generate ultrasensitivity under physiologically plausible conditions

To investigate whether the requirement of the strong sequestration can be relaxed by adding the displacement-type repression, we expanded the model where the complex R_A can dissociate from DNA with a dissociation constant of K_d (figure 2*g*; see Methods for details). Due to the displacement, E_F is affected by two different reversible bindings between R_A and E_F as well as between A and E_F unlike in the previous models. Thus, the steady state equation of E_F is switched to $AE_F + R_AE_F = K_aE_A + K_dE_R$ from $AE_F = K_aE_A$ (see Methods for details). Similarly, the steady state equation of E_R is also switched to $K_bE_R + K_dE_R = RE_A + R_AE_F$ from $K_bE_R = RE_A$. By solving these coupled equations, we can get the ratio of the steady states of E_F, E_A and E_R, i.e. 1: $I(R)A/K_a$: $J(R)(R/K_b)(A/K_a)$, where $I(R) = (K_s + \sigma K_a + R)/(K_s + \sigma K_a + \sigma R)$ and $J(R) = (K_s + K_a + R)/(K_s + \sigma K_a + \sigma R)$, and $\sigma = K_sK_d/K_bK_a$. Note that when $\sigma = 1$, which is known as the detailed balance condition [40], $I(R) = J(R) = 1$ and thus the ratio becomes the same as the previous simple one. This is because under the detailed balance condition, all reversible bindings reach equilibrium, and thus the steady state equations of the species affected by multiple reversible reactions (e.g. $AE_F + R_AE_F = K_aE_A + K_dE_R$) can be partitioned into the equilibrium relations for each reversible reaction (i.e. $AE_F = K_aE_A$ and $R_AE_F = K_dE_R$) [40]. Therefore, under the detailed balance condition, the transcriptional repression by the three types of repressions becomes equivalent to the repression by the blocking and sequestration types.

When $\sigma \neq 1$, the ratio of the steady states of E_F, E_A and E_R are changed and thus we get $E_A/E_T = I(R)(A/K_a)/(1 + I(R)(A/K_a) + J(R)(R/K_b)(A/K_a))$, different from equation (2.1). After substituting equation (2.3) into A and R and normalizing the variables and parameters with A_T, we can derive the approximation for E_A/E_T in terms of the molar ratio ($\tilde{R}_T$):

$$\frac{E_A}{E_T} \approx \frac{\tilde{I}(\tilde{R}_T)(\tilde{A}(\tilde{R}_T)/\tilde{K}_a)}{1 + \tilde{I}(\tilde{R}_T)(\tilde{A}(\tilde{R}_T)/\tilde{K}_a) + \tilde{J}(\tilde{R}_T)(\tilde{R}(\tilde{R}_T)/\tilde{K}_b)(\tilde{A}(\tilde{R}_T)/\tilde{K}_a)}, \tag{2.5}$$

where $\tilde{I}(\tilde{R}_T) = (\tilde{K}_s + \sigma\tilde{K}_a + \tilde{R}(\tilde{R}_T))/(\tilde{K}_s + \sigma\tilde{K}_a + \sigma\tilde{R}(\tilde{R}_T))$, $\tilde{J}(\tilde{R}_T) = (\tilde{K}_s + \tilde{K}_a + \tilde{R}(\tilde{R}_T))/(\tilde{K}_s + \sigma\tilde{K}_a + \sigma\tilde{R}(\tilde{R}_T))$, and $\tilde{X} = X/A_T$ ($X \in \{A, R, K_a, K_b, K_s, K_d\}$). To investigate whether the displacement enhances the sensitivity of the transcriptional activity, we first consider the case where R binds to the free A and the DNA-bound A with the same affinity (i.e. $\tilde{K}_b = \tilde{K}_s$), so the combination of the sequestration- and blocking-type repressions fails to generate the ultrasensitivity (figure 2*f* and electronic supplementary material, figure S1). In this case, if R_A and A have the same binding affinity with DNA (i.e. $\tilde{K}_d = \tilde{K}_a$), $\sigma = 1$ and thus the displacement-type repression does not make any difference compared to the combination of the sequestration- and blocking-type repressions (figure 2*e*,*h*, dashed lines). On the other hand, if effective displacement occurs (i.e. R_A more easily dissociates from DNA compared to A, $\tilde{K}_d > \tilde{K}_a$), E_R decreases and E_A increases. As a result, the higher level of transcriptional activity is maintained until $\tilde{R}_T$ becomes closer to one, yielding greater sensitivity (figure 2*h*, solid line). Consistently, the effective Hill coefficient becomes larger as $\tilde{K}_d$ becomes greater than $\tilde{K}_a$ (figure 2*i*). Furthermore, even if $\tilde{K}_b < \tilde{K}_s$ (i.e. the sequestration is weaker than the blocking), the ultrasensitivity can be generated when the effective displacement occurs (electronic supplementary material, figure S2), unlike with the combination of blocking and sequestration (figure 2*f* and electronic supplementary material, figure S1). Taken together, effective displacement can eliminate the requirement for the combination of the sequestration- and blocking-type repressions to generate the ultrasensitivity.

When there is no energy expenditure, the dissociation constants have to satisfy the detailed balance condition ($\sigma = \tilde{K}_s\tilde{K}_d/\tilde{K}_b\tilde{K}_a = 1$) [41]. In this case, effective displacement can occur ($\tilde{K}_d > \tilde{K}_a$) under limited conditions ($\tilde{K}_s < \tilde{K}_b$), which is challenging to achieve physiologically. On the other hand, when energy is expended to break the detailed balance condition ($\sigma > 1$), effective displacement can occur without the limitation. Such energy expenditure can happen mechanistically by adenosine triphosphate hydrolysis [42].

Interestingly, when there is no energy expenditure to break the detailed balance condition, the equilibrium relations for each reversible reaction (i.e. $AE_F = K_aE_A$, $R_AE_F = K_dE_R$) hold at the steady state [40]. Thus, the transcription regulated by all three repressions becomes the same as that regulated by any two of the repressions (see electronic supplementary material for details). This allows us to easily identify the condition for ultrasensitivity generated with any two repression mechanisms by substituting the detailed balance condition ($\sigma = \tilde{K}_s\tilde{K}_d/\tilde{K}_b\tilde{K}_a = 1$) to the condition for the ultrasensitivity generated with the three repression mechanisms (electronic supplementary material, table S1). This reveals that the requirement of strong sequestration of the blocking and sequestration model, which was challenging physiologically, is switched to the effective displacement of the blocking and displacement model. Importantly, with energy expenditure, the combination of all three repressions can generate ultrasensitivity over a wider range of conditions compared to the

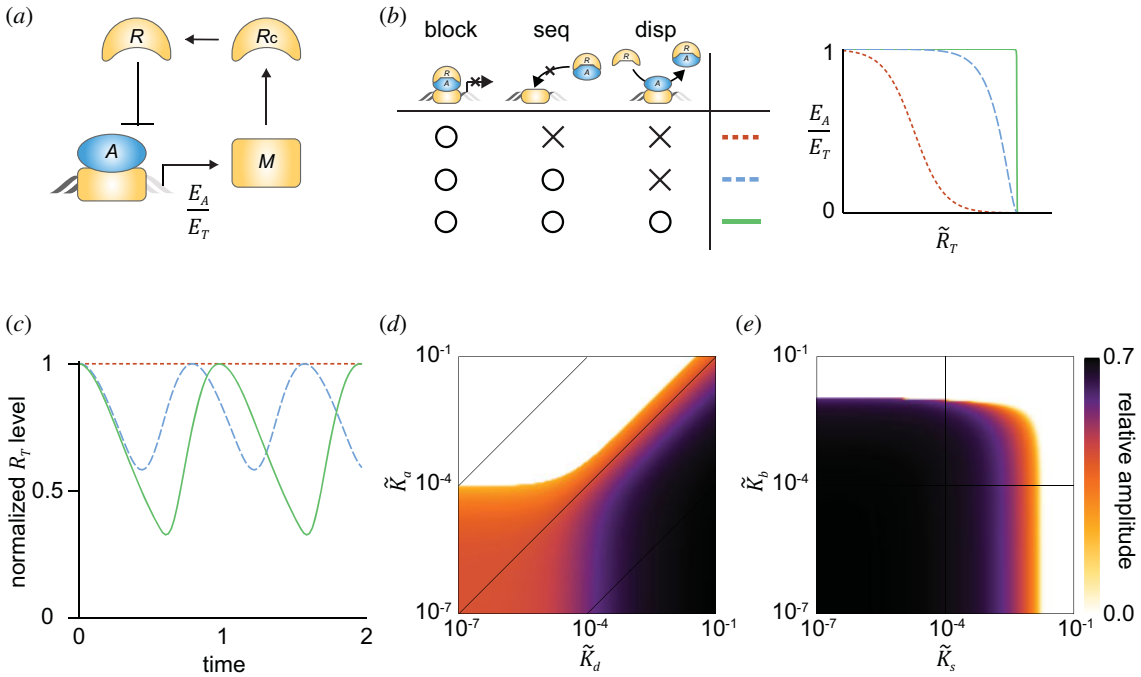

Figure 3. The transcriptional NFL with multiple repression mechanisms can generate strong oscillations. (*a*) In the transcriptional NFL model, the transcription rate of mRNA (M) is determined by the transcriptional activity (E_A/E_T). (*b*) E_A/E_T changes more sensitively in response to $\tilde{R}_T$ when more repression mechanisms are used, as shown in figure 2. (*c*) The NFL model with the sole blocking cannot generate rhythms (red dotted line), while the model with the multiple repressions can generate rhythms (blue dashed and green solid lines). In particular, the combination of the blocking, sequestration, and displacement can generate the strongest rhythms. Here, $A_T = 0.05$, $\tilde{K}_a = 10^{-4}$, $\tilde{K}_b = 10^{-5}$, $\tilde{K}_s = 10^{-5}$ and $\tilde{K}_d = 10^{-1}$ are used, and all trajectories are normalized by their own maximum value to compare their relative amplitudes. (*d*) As the displacement becomes ineffective (i.e. $\tilde{K}_d$ becomes smaller than $\tilde{K}_a$), the relative amplitude decreases. (*e*) Similarly, as the blocking or sequestration becomes weaker (i.e. $\tilde{K}_b$ or $\tilde{K}_s$ increases), the relative amplitude decreases.

combination of any two repressions (figure 2*i*; electronic supplementary material, table S1 and figures S2 and S3).

2.4. The transcriptional negative feedback loop with multiple repression mechanisms can generate strong rhythms

Ultrasensitivity is critical for the transcriptional NFL to generate sustained and strong oscillations [18–21]. Thus, when the transcriptional repression is regulated by the combination of the multiple repression mechanisms, the strong oscillations can be generated. To investigate this, we constructed a simple transcriptional NFL model (figure 3*a*), where the free activator (A) binds to the free DNA, and then promotes the transcription of the repressor mRNA (M). M is translated to the repressor protein in the cytoplasm (R_c). After translocation to the nucleus, the repressor protein (R) inhibits its own transcriptional activator (A) with the previously described repression mechanisms (figure 2*a*,*d*,*g*). Thus, the transcription of M depends on the transcriptional activity E_A/E_T. We assumed that E_A/E_T rapidly reaches its quasi-steady-state because the reversible bindings regulating the transcriptional activity typically occur much faster than the other processes of the transcriptional NFL (i.e. transcription, translation, translocation and degradation). Using the quasi-steady-state approximation (QSSA) and the non-dimensionalization, we can obtain a simple NFL model (see electronic supplementary material for details):

$$\frac{dM}{dt} = \frac{E_A(\tilde{R}_T)}{E_T} - M, \quad \frac{dR_c}{dt} = M - R_c,$$
$$\frac{dR_T}{dt} = R_c - R_T, \tag{2.6}$$

where $E_A(\tilde{R}_T)/E_T$ is the QSSA for the transcriptional activity. Depending on the repression mechanism, we can use the steady state equations for E_A/E_T derived in the previous sections (i.e. equations (2.2), (2.4) and (2.5)). Note that these QSSAs are known as the 'total' QSSAs as they are determined by the molar ratio between the 'total' concentrations of the repressor and activator, $\tilde{R}_T = R_T/A_T$, which is not affected by the fast reversible bindings. Thus, the QSSAs are accurate as long as the reversible bindings are fast [43]. In this way, the NFL model (equation (2.6)) can accurately capture the dynamics of the interactions between A and R even when their levels are comparable [43].

As more repression mechanisms are added, $E_A(\tilde{R}_T)/E_T$ more sensitively changes in response to the variation of $\tilde{R}_T$ (figure 3*b*), which is critical for amplitude amplification. Thus, stronger rhythms, which have a high relative amplitude (i.e. the amplitude normalized by the peak value of the rhythm), are generated (figure 3*c*). Specifically, while the NFL with the sole blocking repression cannot generate rhythms (figure 3*c*, red dotted line), the NFL with the combination of the blocking, sequestration, and displacement can generate the strongest rhythms (figure 3*c*, green solid line). Such strong rhythms become weaker as the displacement becomes ineffective (i.e. $\tilde{K}_d$ becomes smaller than $\tilde{K}_a$; figure 3*d*), or the blocking or the sequestration become weaker (i.e. $\tilde{K}_b$ or $\tilde{K}_s$ increases; figure 3*e*).

2.5. In the mammalian circadian clock, the disruption of synergistic multiple repressions weakens rhythms

In the transcriptional NFL of the mammalian circadian clock, the transcriptional repression occurs via the combination

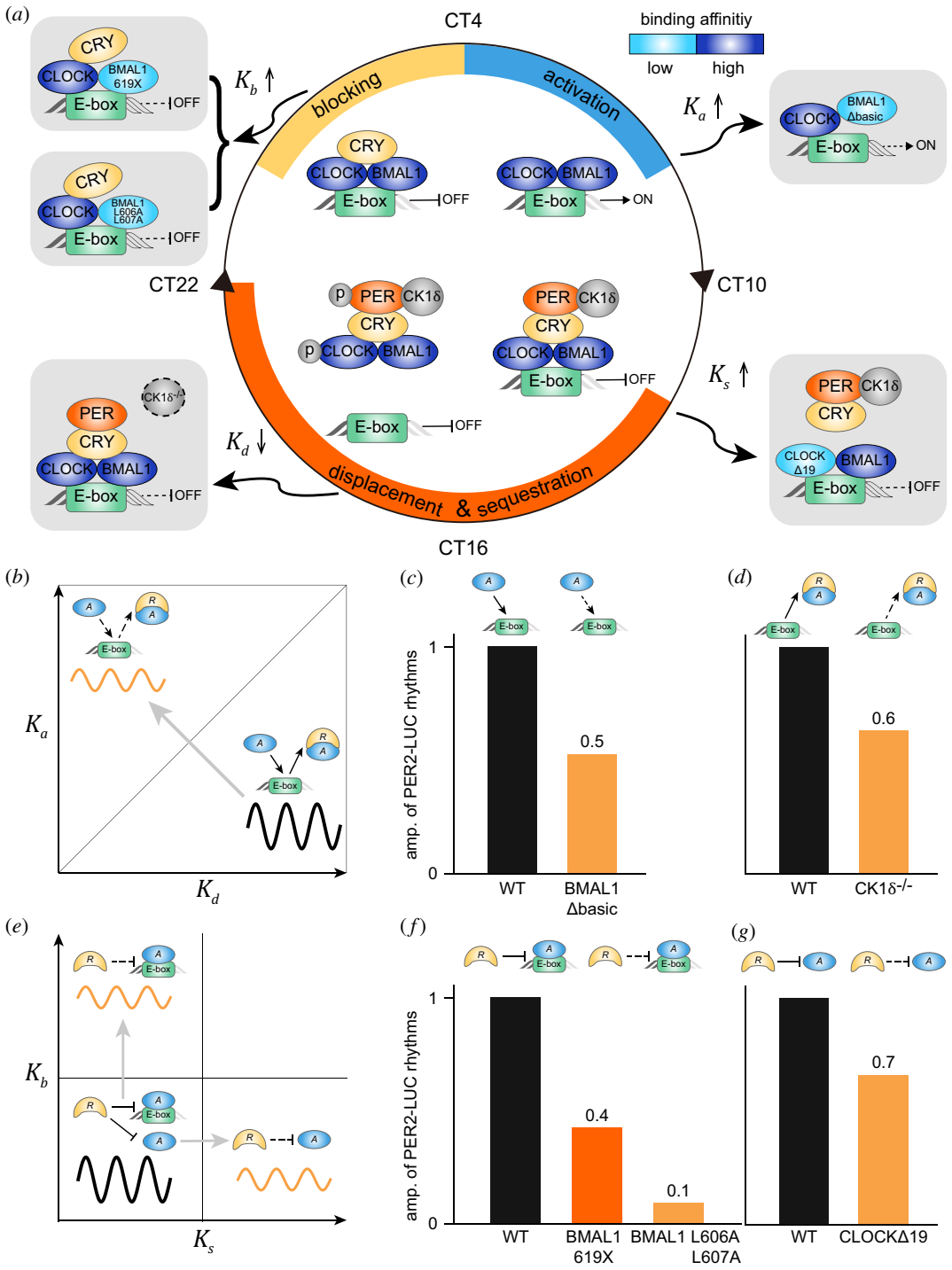

Figure 4. In the mammalian circadian clock, the disruption of synergistic multiple repressions weakens rhythms. (*a*) In the mammalian circadian clock, the transcriptional activity of CLOCK:BMAL1 is regulated by blocking-, sequestration- and displacement-type repressions. Several mutations disrupting the combination of multiple repressions have been identified. BMAL1 transactivation domain mutations such as 619X and L606A L607A decrease the binding affinity between BMAL1 and CRY1 (i.e. K_b increases), weakening the blocking. CLOCKΔ19 has impaired binding with PER (i.e. K_s increase), disrupting the sequestration. A CK1$\delta^{-/-}$ mutation prevents the CK1δ-induced phosphorylation of CLOCK:BMAL1, which is essential for the effective displacement (i.e. K_d decreases). Furthermore, BMAL1Δbasic has impaired binding with the E-box (i.e. K_a increases), decreasing K_d/K_a and thus disrupting the effective displacement. (*b*) Schematic diagram showing the alteration of amplitudes by change in dissociation constants K_a and K_d based on the predictions in figure 3*d*. In the mammalian circadian clock, CLOCK:BMAL1 shows higher binding affinity with the E-box compared to the PER:CRY:CLOCK:BMAL1 complex (i.e. $K_d/K_a > 1$; below the grey line) [15], which is critical for strong rhythm generation according to our model prediction. (*c*,*d*) When K_a was increased by the BMAL1Δbasic mutation (*c*) and K_d was decreased by the CK1$\delta^{-/-}$ mutation (*d*), the amplitude of PER2-LUC rhythms was reduced to 0.5 and 0.6 compared to WT mice, respectively. Adapted from [36] and [33]. (*e*) Schematic diagram showing the alteration of amplitudes by change in dissociation constants K_s and K_b based on the predictions in figure 3*e*. In the mammalian circadian clock, PER:CRY binds with CLOCK:BMAL1 tightly (i.e. small K_s) and CRY binds with CLOCK:BMAL1:E-box tightly (i.e. small K_b), which is crucial for strong rhythm generation according to our model prediction. (*f*) Indeed, as the dissociation constant between CRY and CLOCK:BMAL1:E-box (K_b) was increased by the BMAL1 619X mutation, the amplitude of PER2-LUC rhythms from fibroblasts in mutant mice was reduced to 0.4 compared to that in WT. The amplitude was further reduced when K_b was further increased by the BMAL1 L606A L607A mutation. Adapted from [35]. (*g*) When the binding affinity between PER and CLOCK was decreased (i.e. K_s increased) by the CLOCKΔ19 mutation, the amplitude of PER2-LUC rhythms in the SCN of mutant mice was reduced to 0.7 compared to that in WT mice. Adapted from [34]. For each mutation, all adapted PER2-LUC rhythms of WT and mutant mice were measured under the same condition. However, amplitudes among different mutations cannot be compared due to different experimental conditions.

of blocking, sequestration and displacement (figure 4*a*). Specifically, CLOCK:BMAL1 binding to E-box regulatory elements in the Period (Per1 and Per2) and Cryptochrome (Cry1 and Cry2) genes activates their transcription at around circadian time (CT) 4–8. After CRY and PER are translated in the cytoplasm, they form the complex with the kinase CK1δ and enter the nucleus. The complex dissociates CLOCK:BMAL1 from the E-box and sequesters CLOCK:BMAL1 to prevent binding to the E-box at around CT12–22 (displacement- and sequestration-type repression). At around CT0–4, CRY binds to the CLOCK:BMAL1:E-box complex to block the transcriptional activity (blocking-type repression) [15–17,44].

In the mammalian circadian clock, because the PER:CRY complex recruits CK1δ, inducing dissociation of CLOCK:BMAL1 from the E-box [15], the binding affinity of CLOCK:BMAL1 with the E-box is higher compared to its complex with PER:CRY (i.e. $K_d/K_a > 1$). This effective displacement is critical for strong rhythm generation (figure 4*b*, black solid line) according to our model prediction (figure 3*d*). Then we can expect that, as either K_a increases or K_d decreases (i.e. K_d/K_a decreases), which deactivates the displacement-type repression, the circadian rhythms become weaker (figure 4*b*, orange solid line). Indeed, when K_a was increased by a BMAL1 mutant lacking the basic region (BMAL1Δbasic), which is critical for the binding of BMAL1 to the E-box element (figure 4*a*, top right), the amplitude of PER2-LUC rhythms from the fibroblasts of mutant mice was reduced compared to that from wild-type (WT) mice (figure 4*c*) [36]. Furthermore, when K_d was decreased by a CK1$\delta^{-/-}$ mutant lacking the CK1δ-induced dissociation of CLOCK:BMAL1 from the E-box (figure 4*a*, bottom left), the amplitude of PER2-LUC rhythms in the suprachiasmatic nucleus (SCN) of mutant mice was also reduced compared to that in WT mice (figure 4*d*) [33]. Note that the amplitude reduction by the CK1$\delta^{-/-}$ mutant could be due to other factors because CK1δ also regulates the stability and nucleus entry of PER [45].

The blocking- and sequestration-type repressions also effectively occur in the mammalian circadian clock. That is, PER:CRY binds with CLOCK:BMAL1 tightly (i.e. small K_s), and CRY binds with CLOCK:BMAL1:E-box tightly (i.e. small K_b) [46]. Such tight bindings are important for strong rhythm generation (figure 4*e*, black solid line) according to our model prediction (figure 3*e*). Thus, as either K_b or K_s increases, weakening the blocking- or the sequestration-type repression, the rhythms are expected to become weaker (figure 4*e*, orange solid lines). Indeed, when K_b was increased due to the BMAL1 619X mutation reducing the binding affinity between BMAL1 and CRY1 (figure 4*a*, top left), the amplitude of PER2-LUC rhythms from the fibroblasts of mutant mice was reduced to 0.4 compared to WT (figure 4*f*) [35]. When K_b was further increased by a BMAL1 L606A L607A mutation, the amplitude was further reduced (figure 4*f*) [35]. Moreover, when K_s was increased by the CLOCK mutant lacking the exon 19 region (CLOCKΔ19), which is required for the binding of PER (figure 4*a*, bottom right) [47], the amplitude of PER2-LUC rhythms in the SCN of mutant mice was reduced compared to that in WT mice (figure 4*g*) [34]. Note that such reduction of the amplitude by CLOCKΔ19 could be due to other factors such as the low transcriptional activity of CLOCKΔ19 [48] and the impaired binding with the E-box [49].

3. Discussion

Transcriptional repression plays a central role in precisely regulating gene expression [2]. Various mechanisms for the repression have been identified [2–4]. In particular, the transcriptional activators can be inhibited in various ways by repressors such as blocking, sequestration and displacement (figure 1*a*). Interestingly, these repression mechanisms are used together to inhibit a transcriptional activator in many biological systems [3]. In this study, we found that multiple repression mechanisms can synergistically generate a sharply ultrasensitive transcriptional response (figure 2) and thus strong rhythms in the transcriptional NFL (figure 3). Consistently, the mutations disrupting any of the blocking, sequestration or displacement in the transcriptional NFL of the mammalian circadian clock weaken the circadian rhythms (figure 4). Our work identifies a benefit of using multiple repression mechanisms together, the emergence of ultrasensitive responses, which are critical for cellular regulation such as epigenetic switches, the cell cycle and circadian clocks [22].

Recently, detailed transcriptional repression mechanisms underlying various biological systems have been identified. For instance, while MDM2 was known to inhibit p53 by promoting its degradation [50], recent studies have suggested that MDM2 can also inhibit p53 through displacement and blocking [51,52]. In the Rb-E2F bistable switch, the suppressor Rb protein and the E2F family of transcription factors inhibit mutually with multiple repression mechanisms such as blocking and chromatin structure modification, which are critical to generate ultrasensitivity and thus the bistable switch of cell cycle [6,7,53]. However, such repression mechanisms have not yet been incorporated into the mathematical models [54–57]. Similarly, the recent discoveries of multiple repression mechanisms underlying biological oscillators such as the circadian clock [14–17] and the NF-κB oscillator [12,13] have not been fully incorporated even in recent mathematical models [24,58–63]. In particular, the majority of the mathematical models for various systems have used the simple Michaelis–Menten- or Hill-type functions to describe the transcriptional repression regardless of its underlying repression mechanisms, which can distort the dynamics of the system [21,43]. Our work highlights the importance of careful modelling of the transcriptional repression depending on blocking, sequestration or displacement to accurately capture the underlying dynamics.

Interestingly, to fully use the three repression mechanisms, energy expenditure is required. Without the energy expenditure, the detailed balance condition needs to be satisfied ($\sigma = K_sK_d/K_bK_a = 1$). Under this restriction, the transcriptions regulated by the three repression mechanisms and any two of these become equivalent (see electronic supplementary material for details). As a result, the ultrasensitivity is generated under a limited condition compared to when the detailed balance condition is broken via dissipation of energy ($\sigma > 1$) (figure 2*i*; electronic supplementary material, table S1 and figures S1 and S2). Similarly, the limitation for generating the sensitivity of transcription under the detailed balance condition was also identified when DNA is directly regulated by its transcriptional factors [41]. Specifically, Estrada *et al*. found that when the energy expenditure breaks the detailed balance condition, the cooperative

bindings of the transcriptional factors to multiple binding sites of DNA are more likely to generate ultrasensitivity.

The advantages of using multiple repression mechanisms for biological oscillators have just begun to be investigated. For instance, in the NF-κB oscillator, IκBα inhibits its own transcriptional activator NF-κB via sequestration and displacement. Wang *et al*. found that the displacement can enhance NF-κB oscillation by dissociating the NF-κB from decoy sites and promoting its nuclear export (i.e. facilitating the sequestration), and compensating for the heterogeneous binding affinity of NF-κB to the promoter of IκBα [64]. Furthermore, a recent study of the transcriptional NFL of the mammalian circadian clock found that the displacement of the transcriptional activator (BMAL1:CLOCK) by its repressor (PER:CRY) can facilitate the mobility of the BMAL1:CLOCK to its various target sites, pointing out the hidden role of PER:CRY [65]. While PER:CRY dissociates and sequesters CLOCK:BAML1 from E-box (i.e. sequestration and displacement type), CRY blocks the transcriptional activity of CLOCK:BMAL1 (i.e. blocking type) [15–17]. Because Cry1 displays a delayed expression phase compared to Per, the blocking repression occurs at the late phase, which turns out to be critical for rhythm generation [66–68]. It would be interesting in future work to extend the model to include multiple repressors (e.g. PER and CRY) to investigate their distinct roles.

While we focused on transcriptional repression mechanisms, other mechanisms leading to ultrasensitivity [69], and thus generating rhythms, have been identified. For instance, phosphorylation of the repressor [24,70,71] and saturated degradation of the repressor [25,32,72] can be additional sources of ultrasensitivity for strong rhythms. Furthermore, an additional transcriptional positive feedback loop has been known to enhance the robustness of rhythms [18,21,71,73] in the presence of Hill-type transcriptional repression, which can be induced by phosphorylation-based transcriptional repression [74,75]. On the other hand, when the transcription is regulated by sequestration-type repression, an additional NFL rather than the positive feedback loop can enhance the robustness of rhythms [21,28,32]. It would be important in future work to investigate the role of additional feedback loops depending on the transcriptional repression mechanisms identified in this study.

A transcriptional NFL, where a single repressor inhibits its own transcription by binding to its own promoter, is the simplest design of the synthetic genetic oscillator [76,77]. To generate the ultrasensitivity with this simple design, Stricker *et al*. used a repressor that forms a tetramer to bind with its own promoter [78]. Nonetheless, the degree of the ultrasensitivity was not enough for the synthetic oscillator to generate strong oscillations with high amplitude. Thus, more complex designs of synthetic oscillators have been constructed [76,77]: the modified repressilators [79,80], the combination of the negative and positive feedback loops [78,81], and the coupling of synthetic microbial consortia [82–85]. Our study proposes that a strong synthetic oscillator with a simple design (i.e. a single NFL) could be constructed by modifying the previously used repression mechanisms. That is, by using the combining blocking-, sequestration- and displacement-type repressions, although this might be challenging to implement, ultrasensitivity to achieve strong rhythms could be obtained, providing a new strategy for the design of synthetic oscillators.

4. Methods

4.1. The equation for the transcriptional activity regulated by the sole blocking-type repression

The transcription regulated by sole blocking-type repression (figure 2*a*) can be described by the following system of ordinary differential equations (ODEs) based on the mass action law:

$$\left.\begin{aligned}
\frac{dR}{dt} &= -k_{fb}RE_A + k_bE_R,\\
\frac{dA}{dt} &= -k_{fa}AE_F + k_aE_A,\\
\frac{dE_F}{dt} &= -k_{fa}AE_F + k_aE_A,\\
\frac{dE_A}{dt} &= k_{fa}AE_F - k_aE_A - k_{fb}RE_A + k_bE_R\\
\text{and}\quad \frac{dE_R}{dt} &= k_{fb}RE_A - k_bE_R,
\end{aligned}\right\} \tag{4.1}$$

where R, A, E_F, E_A and E_R represent the concentration of the repressor, the activator, DNA, the activator-bound DNA and the activator and repressor complex-bound DNA, respectively. Here, k_{fb} (k_b) and k_{fa} (k_a) are the association (dissociation) rate constants between E_A and R and between A and E_F, respectively. Note that as $\frac{dR}{dt}+\frac{dE_R}{dt}=0$, $\frac{dA}{dt}+\frac{dE_A}{dt}+\frac{dE_R}{dt}=0$ and $\frac{dE_F}{dt}+\frac{dE_A}{dt}+\frac{dE_R}{dt}=0$, the total concentrations of the repressor ($R_T \equiv R+E_R$), the activator ($A_T \equiv A+E_A+E_R$), and DNA ($E_T \equiv E_F+E_A+E_R$) are conserved. The steady states of the system satisfy the following equations:

$$RE_A = K_bE_R,\ AE_F = K_aE_A, \tag{4.2}$$

where $K_b = k_b/k_{fb}$ and $K_a = k_a/k_{fa}$. This yields E_F: E_A: E_R = 1: A/K_a: $(R/K_b)(A/K_a)$, and thus the steady state for E_A/E_T:

$$\frac{E_A}{E_T} = \frac{E_A}{E_F+E_A+E_R} = \frac{E_A/E_F}{1+(E_A/E_F)+(E_R/E_F)} = \frac{A/K_a}{1+(A/K_a)+(R/K_b)(A/K_a)}, \tag{4.3}$$

where A and R in equation (4.3) are the steady states of the free activator and the free repressor, respectively.

Equation (4.3) can be simplified if the total concentration of DNA (E_T) is much lower than the concentrations of the activator (A_T) and repressor (R_T) and thus $A_T = A+E_A+E_R \approx A$ and $R_T = R+E_R \approx R$. That is, by replacing A and R in equation (4.3) with conserved A_T and R_T, respectively, we get the following approximation for equation (4.3):

$$\frac{E_A}{E_T} \approx \frac{A_T/K_a}{1+(A_T/K_a)+(R_T/K_b)(A_T/K_a)}, \tag{4.4}$$

which is accurate as long as E_T/A_T is small (electronic supplementary material, figure S4a). This assumption is likely to hold in the mammalian circadian clock as the number of BMAL1:CLOCK in the mammalian cells is about 10^4–10^5 [38]. On the other hand, it might not be acceptable in *E. coli* or *S. cerevisiae* cells, which contain much lower numbers of transcription factors (10^1–10^2) [38].

4.2. The equation for the transcriptional activity regulated by the blocking- and sequestration-type repressions

The transcription regulated by both blocking and sequestration (figure 2*d*) can be described by the following ODEs:

$$\left.\begin{aligned}
\frac{dR}{dt} &= -k_{fb}RE_A + k_bE_R - k_{fs}RA + k_sR_A,\\
\frac{dA}{dt} &= -k_{fa}AE_F + k_aE_A - k_{fs}RA + k_sR_A,\\
\frac{dR_A}{dt} &= k_{fs}RA - k_sR_A,\\
\frac{dE_F}{dt} &= -k_{fa}AE_F + k_aE_A,\\
\frac{dE_A}{dt} &= k_{fa}AE_F - k_aE_A - k_{fb}RE_A + k_bE_R\\
\text{and}\quad \frac{dE_R}{dt} &= k_{fb}RE_A - k_bE_R.
\end{aligned}\right\} \tag{4.5}$$

The reversible binding between R and A to form the complex (R_A) with the association rate constant k_{fs} and the dissociation rate constant k_s are added to equation (4.1). Thus, the conservation laws for the activator and the repressor are changed to $A_T = A + R_A + E_A + E_R$ and $R_T = R + R_A + E_R$, respectively. Because the steady states of equation (4.5) also satisfy equation (4.2), the steady state of E_A/E_T in this system also satisfies equation (4.3). However, even if E_T is much lower than A_T and R_T, equation (4.3) cannot be simplified by replacing A and R with A_T and R_T because $A_T = A + R_A + E_A + E_R \approx A + R_A$ and $R_T = R + R_A + E_R \approx R + R_A$. Thus, we also need to use another steady state equation, $AR = K_sR_A$, where $K_s = k_s/k_{fs}$, to derive the steady state of R_A in terms of A_T and R_T. Specifically, by replacing A and R with $A_T - R_A$ and $R_T - R_A$, respectively, in $AR = K_sR_A$, we get $R_A^2 - (A_T + R_T + K_s)R_A + A_TR_T \approx 0$, yielding the approximate steady state for R_A:

$$R_A \approx \frac{A_T + R_T + K_s - \sqrt{(A_T - R_T - K_s)^2 + 4A_TK_s}}{2}. \tag{4.6}$$

Then by substituting equation (4.6) to $A \approx A_T - R_A$ and $R \approx R_T - R_A$, we can get the following approximate steady state for the free activator and repressor:

$$\begin{aligned}
A &\approx \frac{A_T - R_T - K_s + \sqrt{(A_T - R_T - K_s)^2 + 4A_TK_s}}{2},\\
R &\approx \frac{R_T - A_T - K_s + \sqrt{(A_T - R_T - K_s)^2 + 4A_TK_s}}{2}.
\end{aligned} \tag{4.7}$$

By substituting equation (4.7) to equation (4.3), the approximate E_A/E_T can be derived (equation (2.4)), which is accurate as long as E_T/A_T is small (electronic supplementary material, figure S4b).

4.3. The equation for the transcriptional activity regulated by all the blocking-, sequestration- and displacement-type repressions

The transcription regulated by all blocking, sequestration, and displacement (figure 2*g*) can be described by the following ODEs:

$$\left.\begin{aligned}
\frac{dR}{dt} &= -k_{fb}RE_A + k_bE_R - k_{fs}RA + k_sR_A,\\
\frac{dA}{dt} &= -k_{fa}AE_F + k_aE_A - k_{fs}RA + k_sR_A,\\
\frac{dR_A}{dt} &= k_{fs}RA - k_sR_A - k_{fd}R_AE_F + k_dE_R,\\
\frac{dE_F}{dt} &= -k_{fa}AE_F + k_aE_A - k_{fd}R_AE_F + k_dE_R,\\
\frac{dE_A}{dt} &= k_{fa}AE_F - k_aE_A - k_{fb}RE_A + k_bE_R\\
\text{and}\quad \frac{dE_R}{dt} &= k_{fb}RE_A - k_bE_R + k_{fd}R_AE_F - k_dE_R,
\end{aligned}\right\} \tag{4.8}$$

which have the same conservation laws as equation (4.5). Because the reversible binding between R_A and E_F to form E_R with the association rate constant k_{fd} and the dissociation rate constant k_d are added to equation (4.5), the steady states are changed to the following equations:

$$\left.\begin{aligned}
RA - K_sR_A - \gamma(R_AE_F - K_dE_R) &= 0,\\
AE_F - K_aE_A - \delta(RE_A - K_bE_R) &= 0\\
\text{and}\quad RE_A - K_bE_R + \theta(R_AE_F - K_dE_R) &= 0,
\end{aligned}\right\} \tag{4.9}$$

where $K_d = k_d/k_{fd}$, $\gamma = k_{fd}/k_{fs}$, $\delta = k_{fb}/k_{fa}$, and $\theta = k_{fd}/k_{fb}$. If E_T is much lower than A_T and R_T, and thus $A_T = A + R_A + E_A + E_R \approx A + R_A$ and $R_T = R + R_A + E_R \approx R + R_A$, the last two equations of (4.9) can be simplified as follows:

$$\left.\begin{aligned}
(A_T - R_A)(E_T - E_A - E_R) - K_aE_A - \delta(R_T - R_A)E_A + \delta K_bE_R &\approx 0,\\
(R_T - R_A)E_A - K_bE_R + \theta R_A(E_T - E_A - E_R) - \theta K_dE_R &\approx 0.
\end{aligned}\right\} \tag{4.10}$$

Their solution yields the steady state approximation for E_A/E_T as

$$\frac{(\theta R_A + K_b + \theta K_d)(R_A - A_T) - \theta(R_A - A_T + \delta K_b)R_A}{((1+\delta)R_A - A_T - \delta R_T - K_a)(\theta R_A + K_b + \theta K_d) - (R_A - A_T + \delta K_b)((\theta+1)R_A - R_T)}. \tag{4.11}$$

Furthermore, by using the approximation $A_T \approx A + R_A$ and $R_T \approx R + R_A$, we can simplify the first equation of equation (4.9) as follows:

$$R_A^2 - (A_T + R_T + K_s - \gamma E_F)R_A + A_TR_T - \gamma K_dE_R \approx 0. \tag{4.12}$$

Because E_T is much lower than A_T and R_T, equation (4.12) can be further simplified to $R_A^2 - (A_T + R_T + K_s)R_A + A_TR_T \approx 0$, leading to the approximation for the steady state of R_A described in equation (4.6). Then, by substituting equation (4.6) to equation (4.11), the approximated E_A/E_T in terms of conserved A_T and R_T can be derived. The approximation of E_A/E_T can be further simplified as follows if we assume $\delta = 1$ and $\theta = 1$ (i.e. the binding rates are the same):

$$\begin{aligned}
\frac{E_A}{E_T} &\approx \frac{(R_A + K_b + K_d)(R_A - A_T) - (R_A - A_T + K_b)R_A}{(2R_A - A_T - R_T - K_a)(R_A + K_b + K_d) - (R_A - A_T + K_b)(2R_A - R_T)}\\
&= \frac{(K_b + K_d)A_T - K_dR_A}{[(K_b + K_d)K_a + K_d(R_T - R_A)] + [(K_b + K_d)A_T - K_dR_A] + [(R_T - R_A)A_T + K_aR_A]}.
\end{aligned} \tag{4.13}$$

Each term of equation (4.13) can be transformed by using $A \approx A_T - R_A$, $R \approx R_T - R_A$, and $AR \approx K_s R_A$ as follows:

$$\left.\begin{aligned}
&(K_b + K_d)K_a + K_d(R_T - R_A) \approx K_b K_a + K_d K_a + K_d R = \mu(K_s + \sigma K_a + \sigma R),\\
&(K_b + K_d)A_T - K_d R_A \approx (K_b + K_d)(A + R_A) - K_d R_A \approx K_b A + K_d A + \frac{K_b}{K_s} RA = \mu(K_s + \sigma K_a + R)\frac{A}{K_a},\\
&(R_T - R_A)A_T + K_a R_A \approx R\left(A + \frac{RA}{K_s}\right) + K_a \frac{RA}{K_s} = \mu(K_s + K_a + R)\frac{R}{K_b}\frac{A}{K_a},
\end{aligned}\right\} \tag{4.14}$$

where $\sigma = K_s K_d / K_b K_a$ and $\mu = K_b K_a / K_s$. By substituting equation (4.14) to equation (4.13), we can derive equation (2.5) as follows:

$$\begin{aligned}
\frac{E_A}{E_T} &\approx \frac{(K_s + \sigma K_a + R)A/K_a}{(K_s + \sigma K_a + \sigma R) + (K_s + \sigma K_a + R)A/K_a + (K_s + K_a + R)(R/K_b)(A/K_a)}\\
&= \frac{I(R)A/K_a}{1 + I(R)(A/K_a) + J(R)(R/K_b)(A/K_a)},
\end{aligned} \tag{4.15}$$

where $I(R) = (K_s + \sigma K_a + R)/(K_s + \sigma K_a + \sigma R)$ and $J(R) = (K_s + K_a + R)/(K_s + \sigma K_a + \sigma R)$. By substituting equation (4.7) into A and R and then normalizing the variables and parameters with A_T, we can derive the approximated equation (2.5) for E_A/E_T in terms of the molar ratio R_T. This approximation is accurate as long as E_T/A_T is small (electronic supplementary material, figure S4c). Importantly, it accurately captures the cases when δ and θ are not one if the displacement effectively occurs ($K_d > K_a$; electronic supplementary material, figure S5).

Data accessibility. This article has no additional data.

Authors' contributions. E.M.J.: conceptualization, formal analysis, methodology, validation, visualization, writing—original draft, writing—review and editing; Y.M.S.: data curation, formal analysis, methodology, visualization, writing—original draft, writing—review and editing; J.K.K.: conceptualization, data curation, formal analysis, funding acquisition, methodology, supervision, visualization, writing—original draft, writing—review and editing.

All authors gave final approval for publication and agreed to be held accountable for the work performed therein.

Competing interests. We declare we have no competing interests.

Funding. This work was supported by the Human Frontiers Science Program Organization (grant no. RGY0063/2017) (J.K.K.); the National Research Foundation of Korea, Ministry of Science and ICT (grant no. NRF-2016 RICIB 3008468) (J.K.K.); and the Institute for Basic Science (grant no. IBS-R029-C3) (J.K.K.).

References

1. Ma J. 2011 Transcriptional activators and activation mechanisms. *Protein Cell* **2**, 879–888. (doi:10.1007/s13238-011-1101-7)
2. Maldonado E, Hampsey M, Reinberg D. 1999 Repression: targeting the heart of the matter. *Cell* **99**, 455–458. (doi:10.1016/s0092-8674(00)81533-0)
3. Gaston K, Jayaraman PS. 2003 Transcriptional repression in eukaryotes: repressors and repression mechanisms. *Cell. Mol. Life Sci.* **60**, 721–741. (doi:10.1007/s00018-003-2260-3)
4. Renkawitz R. 1990 Transcriptional repression in eukaryotes. *Trends Genet.* **6**, 192–197. (doi:10.1016/0168-9525(90)90176-7)
5. Luo RX, Postigo AA, Dean DC. 1998 Rb interacts with histone deacetylase to repress transcription. *Cell* **92**, 463–473. (doi:10.1016/s0092-8674(00)80940-x)
6. Nevins JR. 1992 E2F: a link between the Rb tumor suppressor protein and viral oncoproteins. *Science* **258**, 424–429. (doi:10.1126/science.1411535)
7. Dimova DK, Dyson NJ. 2005 The E2F transcriptional network: old acquaintances with new faces. *Oncogene* **24**, 2810–2826. (doi:10.1038/sj.onc.1208612)
8. Kaffman A, Rank NM, O'Neill EM, Huang LS, O'Shea EK. 1998 The receptor Msn5 exports the phosphorylated transcription factor Pho4 out of the nucleus. *Nature* **396**, 482–486. (doi:10.1038/24898)
9. Kaffman A, Herskowitz I, Tjian R, O'Shea EK. 1994 Phosphorylation of the transcription factor PHO4 by a cyclin-CDK complex, PHO80-PHO85. *Science* **263**, 1153–1156. (doi:10.1126/science.8108735)
10. Jayaraman PS, Hirst K, Goding CR. 1994 The activation domain of a basic helix-loop-helix protein is masked by repressor interaction with domains distinct from that required for transcription regulation. *EMBO J.* **13**, 2192–2199.
11. Ghosh S, May MJ, Kopp EB. 1998 NF-kappa B and Rel proteins: evolutionarily conserved mediators of immune responses. *Annu. Rev. Immunol.* **16**, 225–260. (doi:10.1146/annurev.immunol.16.1.225)
12. Bergqvist S, Alverdi V, Mengel B, Hoffmann A, Ghosh G, Komives EA. 2009 Kinetic enhancement of NF-kappaBxDNA dissociation by IkappaBalpha. *Proc. Natl Acad. Sci. USA* **106**, 19 328–19 333. (doi:10.1073/pnas.0908797106)
13. Potoyan DA, Zheng W, Komives EA, Wolynes PG. 2016 Molecular stripping in the NF-kappaB/IkappaB/DNA genetic regulatory network. *Proc. Natl Acad. Sci. USA* **113**, 110–115. (doi:10.1073/pnas.1520483112)
14. Menet JS, Abruzzi KC, Desrochers J, Rodriguez J, Rosbash M. 2010 Dynamic PER repression mechanisms in the *Drosophila* circadian clock: from on-DNA to off-DNA. *Genes Dev.* **24**, 358–367. (doi:10.1101/gad.1883910)
15. Cao X, Yang Y, Selby CP, Liu Z, Sancar A. 2021 Molecular mechanism of the repressive phase of the mammalian circadian clock. *Proc. Natl Acad. Sci. USA* **118**, e2021174118. (doi:10.1073/pnas.2021174118)
16. Chiou YY, Yang Y, Rashid N, Ye R, Selby CP, Sancar A. 2016 Mammalian Period represses and de-represses transcription by displacing CLOCK-BMAL1 from promoters in a Cryptochrome-dependent manner. *Proc. Natl Acad. Sci. USA* **113**, E6072–E6079. (doi:10.1073/pnas.1612917113)
17. Ye R, Selby CP, Chiou YY, Ozkan-Dagliyan I, Gaddameedhi S, Sancar A. 2014 Dual modes of CLOCK: BMAL1 inhibition mediated by Cryptochrome and

Period proteins in the mammalian circadian clock. *Genes Dev.* **28**, 1989–1998. (doi:10.1101/gad.249417.114)

18. Novak B, Tyson JJ. 2008 Design principles of biochemical oscillators. *Nat. Rev. Mol. Cell Biol.* **9**, 981–991. (doi:10.1038/nrm2530)
19. Ferrell Jr JE, Tsai TY, Yang Q. 2011 Modeling the cell cycle: why do certain circuits oscillate? *Cell* **144**, 874–885. (doi:10.1016/j.cell.2011.03.006)
20. Ferrell Jr JE, Ha SH. 2014 Ultrasensitivity part III: cascades, bistable switches, and oscillators. *Trends Biochem. Sci.* **39**, 612–618. (doi:10.1016/j.tibs.2014.10.002)
21. Kim JK. 2016 Protein sequestration versus Hill-type repression in circadian clock models. *IET Syst. Biol.* **10**, 125–135. (doi:10.1049/iet-syb.2015.0090)
22. Buchler NE, Cross FR. 2009 Protein sequestration generates a flexible ultrasensitive response in a genetic network. *Mol. Syst. Biol.* **5**, 272. (doi:10.1038/msb.2009.30)
23. Buchler NE, Louis M. 2008 Molecular titration and ultrasensitivity in regulatory networks. *J. Mol. Biol.* **384**, 1106–1119. (doi:10.1016/j.jmb.2008.09.079)
24. Beesley S *et al*. 2020 Wake-sleep cycles are severely disrupted by diseases affecting cytoplasmic homeostasis. *Proc. Natl Acad. Sci. USA* **117**, 28 402–28 411. (doi:10.1073/pnas.2003524117)
25. D'Alessandro M *et al*. 2017 Stability of wake-sleep cycles requires robust degradation of the PERIOD protein. *Curr. Biol.* **27**, 3454–3467. (doi:10.1016/j.cub.2017.10.014)
26. Gotoh T, Kim JK, Liu J, Vila-Caballer M, Stauffer PE, Tyson JJ, Finkielstein CV. 2016 Model-driven experimental approach reveals the complex regulatory distribution of p53 by the circadian factor Period 2. *Proc. Natl Acad. Sci. USA* **113**, 13 516–13 521. (doi:10.1073/pnas.1607984113)
27. Kim JK, Kilpatrick ZP, Bennett MR, Josic K. 2014 Molecular mechanisms that regulate the coupled period of the mammalian circadian clock. *Biophys. J.* **106**, 2071–2081. (doi:10.1016/j.bpj.2014.02.039)
28. Kim JK, Forger DB. 2012 A mechanism for robust circadian timekeeping via stoichiometric balance. *Mol. Syst. Biol.* **8**, 630. (doi:10.1038/msb.2012.62)
29. Xie Z, Kulasiri D. 2007 Modelling of circadian rhythms in *Drosophila* incorporating the interlocked PER/TIM and VRI/PDP1 feedback loops. *J. Theor. Biol.* **245**, 290–304. (doi:10.1016/j.jtbi.2006.10.028)
30. Kim JK. 2021 Tick, tock, circadian clocks. In *Case studies in systems biology* (ed. P Kraikivski*)*, pp. 79–94. Cham, Switzerland: Springer International Publishing.
31. Jeong EM, Kwon M, Cho E, Lee SH, Kim H, Kim EY, Kim JK. 2022 Systematic modeling-driven experiments identify distinct molecular clockworks underlying hierarchically organized pacemaker neurons. *Proc. Natl Acad. Sci. USA* **119**, e2113403119. (doi:10.1073/pnas.2113403119)
32. Heidebrecht B, Chen J, Tyson JJ. 2020 Mathematical analysis of robustness of oscillations in models of the mammalian circadian clock. *bioRxiv*, 2020.2009.2015.297648. (doi:10.1101/2020.09.15.297648)
33. Etchegaray JP, Yu EA, Indic P, Dallmann R, Weaver DR. 2010 Casein kinase 1 delta (CK1 delta) regulates period length of the mouse suprachiasmatic circadian clock in vitro. *PLoS ONE* **5**, e10303. (doi:10.1371/journal.pone.0010303)
34. Sujino M, Asakawa T, Nagano M, Koinuma S, Masumoto KH, Shigeyoshi Y. 2018 CLOCKDelta19 mutation modifies the manner of synchrony among oscillation neurons in the suprachiasmatic nucleus. *Sci. Rep.* **8**, 854. (doi:10.1038/s41598-018-19224-1)
35. Xu H, Gustafson CL, Sammons PJ, Khan SK, Parsley NC, Ramanathan C, Lee HW, Liu AC, Partch CL. 2015 Cryptochrome 1 regulates the circadian clock through dynamic interactions with the BMAL1 C terminus. *Nat. Struct. Mol. Biol.* **22**, 476–484. (doi:10.1038/nsmb.3018)
36. Lee Y, Chen RM, Lee HM, Lee C. 2011 Stoichiometric relationship among clock proteins determines robustness of circadian rhythms. *J. Biol. Chem.* **286**, 7033–7042. (doi:10.1074/jbc.M110.207217)
37. Ferrell Jr JE, Ha SH. 2014 Ultrasensitivity part I: Michaelian responses and zero-order ultrasensitivity. *Trends Biochem. Sci.* **39**, 496–503. (doi:10.1016/j.tibs.2014.08.003)
38. Milo R, Phillips R. 2015 *Cell biology by the numbers*. New York, NY: Garland Science.
39. Song YM, Hong H, Kim JK. 2021 Universally valid reduction of multiscale stochastic biochemical systems using simple non-elementary propensities. *PLoS Comput. Biol.* **17**, e1008952. (doi:10.1371/journal.pcbi.1008952)
40. Rubi JM, Bedeaux D, Kjelstrup S, Pagonabarraga I. 2013 Chemical cycle kinetics: removing the limitation of linearity of a non-equilibrium thermodynamic description. *Int. J. Thermophys.* **34**, 1214–1228. (doi:10.1007/s10765-013-1484-1)
41. Estrada J, Wong F, DePace A, Gunawardena J. 2016 Information integration and energy expenditure in gene regulation. *Cell* **166**, 234–244. (doi:10.1016/j.cell.2016.06.012)
42. Qian H. 2007 Phosphorylation energy hypothesis: open chemical systems and their biological functions. *Annu. Rev. Phys. Chem.* **58**, 113–142. (doi:10.1146/annurev.physchem.58.032806.104550)
43. Kim JK, Tyson JJ. 2020 Misuse of the Michaelis-Menten rate law for protein interaction networks and its remedy. *PLoS Comput. Biol.* **16**, e1008258. (doi:10.1371/journal.pcbi.1008258)
44. Partch CL. 2020 Orchestration of circadian timing by macromolecular protein assemblies. *J. Mol. Biol.* **432**, 3426–3448. (doi:10.1016/j.jmb.2019.12.046)
45. Vanselow K *et al.* 2006 Differential effects of PER2 phosphorylation: molecular basis for the human familial advanced sleep phase syndrome (FASPS). *Gene Dev.* **20**, 2660–2672. (doi:10.1101/gad.397006)
46. Kepsutlu B, Kizilel R, Kizilel S. 2014 Quantification of interactions among circadian clock proteins via surface plasmon resonance. *J. Mol. Recognit.* **27**, 458–469. (doi:10.1002/jmr.2367)
47. Lee E, Cho E, Kang DH, Jeong EH, Chen Z, Yoo SH, Kim EY. 2016 Pacemaker-neuron-dependent disturbance of the molecular clockwork by a *Drosophila* CLOCK mutant homologous to the mouse Clock mutation. *Proc. Natl Acad. Sci. USA* **113**, E4904–E4913. (doi:10.1073/pnas.1523494113)
48. Lowrey PL, Takahashi JS. 2011 Genetics of circadian rhythms in mammalian model organisms. *Adv. Genet.* **74**, 175–230. (doi:10.1016/B978-0-12-387690-4.00006-4)
49. Shimomura K *et al*. 2013 *Usf1*, a suppressor of the circadian *Clock* mutant, reveals the nature of the DNA-binding of the CLOCK:BMAL1 complex in mice. *eLife* **2**, e00426. (doi:10.7554/eLife.00426)
50. Haupt Y, Maya R, Kazaz A, Oren M. 1997 Mdm2 promotes the rapid degradation of p53. *Nature* **387**, 296–299. (doi:10.1038/387296a0)
51. Cross B, Chen L, Cheng Q, Li B, Yuan ZM, Chen J. 2011 Inhibition of p53 DNA binding function by the MDM2 protein acidic domain. *J. Biol. Chem.* **286**, 16 018–16 029. (doi:10.1074/jbc.M111.228981)
52. Chen J. 2016 The cell-cycle arrest and apoptotic functions of p53 in tumor initiation and progression. *Cold Spring Harb. Perspect. Med.* **6**, a026104. (doi:10.1101/cshperspect.a026104)
53. Yao G, Lee TJ, Mori S, Nevins JR, You L. 2008 A bistable Rb-E2F switch underlies the restriction point. *Nat. Cell Biol.* **10**, 476–482. (doi:10.1038/ncb1711)
54. Kim E, Kim JY, Lee JY. 2019 Mathematical modeling of p53 pathways. *Int. J. Mol. Sci.* **20**, 5179. (doi:10.3390/ijms20205179)
55. Jolma IW, Ni XY, Rensing L, Ruoff P. 2010 Harmonic oscillations in homeostatic controllers: dynamics of the p53 regulatory system. *Biophys. J.* **98**, 743–752. (doi:10.1016/j.bpj.2009.11.013)
56. Lev Bar-Or R, Maya R, Segel LA, Alon U, Levine AJ, Oren M. 2000 Generation of oscillations by the p53-Mdm2 feedback loop: a theoretical and experimental study. *Proc. Natl Acad. Sci. USA* **97**, 11 250–11 255. (doi:10.1073/pnas.210171597)
57. Monke G, Cristiano E, Finzel A, Friedrich D, Herzel H, Falcke M, Loewer A. 2017 Excitability in the p53 network mediates robust signaling with tunable activation thresholds in single cells. *Sci. Rep.* **7**, 46571. (doi:10.1038/srep46571)
58. Kim R, Reed MC. 2021 A mathematical model of circadian rhythms and dopamine. *Theor. Biol. Med. Model.* **18**, 8. (doi:10.1186/s12976-021-00139-w)
59. Rashid MM, Kurata H. 2020 Coupling protocol of interlocked feedback oscillators in circadian clocks. *J. R. Soc. Interface* **17**, 20200287. (doi:10.1098/rsif.2020.0287)
60. Uriu K, Tei H. 2019 A saturated reaction in repressor synthesis creates a daytime dead zone in circadian clocks. *PLoS Comput. Biol.* **15**, e1006787. (doi:10.1371/journal.pcbi.1006787)
61. Pett JP, Kondoff M, Bordyugov G, Kramer A, Herzel H. 2018 Co-existing feedback loops generate tissue-specific circadian rhythms. *Life Sci. Alliance* **1**, e201800078. (doi:10.26508/lsa.201800078)
62. van Soest I, del Olmo M, Schmal C, Herzel H. 2020 Nonlinear phenomena in models of the circadian clock. *J. R. Soc. Interface* **17**, 20200556. (doi:10.1098/rsif.2020.0556)

63. Almeida S, Chaves M, Delaunay F. 2020 Transcription-based circadian mechanism controls the duration of molecular clock states in response to signaling inputs. *J. Theor. Biol.* **484**, 110015. (doi:10.1016/j.jtbi.2019.110015)
64. Wang Z, Potoyan DA, Wolynes PG. 2016 Molecular stripping, targets and decoys as modulators of oscillations in the NF-kappaB/IkappaBalpha/DNA genetic network. *J. R Soc. Interface* **13**, 20160606. (doi:10.1098/rsif.2016.0606)
65. Bagnall JS *et al*. 2021 Quantification of circadian interactions and protein abundance defines a mechanism for operational stability of the circadian clock. *bioRxiv*, 2021.2008.2027.456017. (doi:10.1101/2021.08.27.456017)
66. Korencic A, Kosir R, Bordyugov G, Lehmann R, Rozman D, Herzel H. 2014 Timing of circadian genes in mammalian tissues. *Sci. Rep.* **4**, 5782. (doi:10.1038/srep05782)
67. Ukai-Tadenuma M, Yamada RG, Xu H, Ripperger JA, Liu AC, Ueda HR. 2011 Delay in feedback repression by cryptochrome 1 is required for circadian clock function. *Cell* **144**, 268–281. (doi:10.1016/j.cell.2010.12.019)
68. Gabriel CH *et al*. 2021 Live-cell imaging of circadian clock protein dynamics in CRISPR-generated knock-in cells. *Nat. Commun.* **12**, 3796. (doi:10.1038/s41467-021-24086-9)
69. Ferrell Jr JE, Ha SH. 2014 Ultrasensitivity part II: multisite phosphorylation, stoichiometric inhibitors, and positive feedback. *Trends Biochem. Sci.* **39**, 556–569. (doi:10.1016/j.tibs.2014.09.003)
70. Tyson JJ, Hong CI, Thron CD, Novak B. 1999 A simple model of circadian rhythms based on dimerization and proteolysis of PER and TIM. *Biophys. J.* **77**, 2411–2417. (doi:10.1016/S0006-3495(99)77078-5)
71. Ananthasubramaniam B, Herzel H. 2014 Positive feedback promotes oscillations in negative feedback loops. *PLoS ONE* **9**, e104761. (doi:10.1371/journal.pone.0104761)
72. Kurosawa G, Iwasa Y. 2002 Saturation of enzyme kinetics in circadian clock models. *J. Biol. Rhythms* **17**, 568–577. (doi:10.1177/0748730402238239)
73. Tsai TY, Choi YS, Ma W, Pomerening JR, Tang C, Ferrell Jr JE. 2008 Robust, tunable biological oscillations from interlinked positive and negative feedback loops. *Science* **321**, 126–129. (doi:10.1126/science.1156951)
74. Gonze D, Abou-Jaoude W. 2013 The Goodwin model: behind the Hill function. *PLoS ONE* **8**, e69573. (doi:10.1371/journal.pone.0069573)
75. Gonze D, Ruoff P. 2021 The Goodwin oscillator and its legacy. *Acta Biotheor.* **69**, 857–874. (doi:10.1007/s10441-020-09379-8)
76. Li Z, Yang Q. 2018 Systems and synthetic biology approaches in understanding biological oscillators. *Quant. Biol.* **6**, 1–14. (doi:10.1007/s40484-017-0120-7)
77. Purcell O, Savery NJ, Grierson CS, di Bernardo M. 2010 A comparative analysis of synthetic genetic oscillators. *J. R. Soc. Interface* **7**, 1503–1524. (doi:10.1098/rsif.2010.0183)
78. Stricker J, Cookson S, Bennett MR, Mather WH, Tsimring LS, Hasty J. 2008 A fast, robust and tunable synthetic gene oscillator. *Nature* **456**, 516–519. (doi:10.1038/nature07389)
79. Potvin-Trottier L, Lord ND, Vinnicombe G, Paulsson J. 2016 Synchronous long-term oscillations in a synthetic gene circuit. *Nature* **538**, 514–517. (doi:10.1038/nature19841)
80. Niederholtmeyer H, Sun ZZ, Hori Y, Yeung E, Verpoorte A, Murray RM, Maerkl SJ. 2015 Rapid cell-free forward engineering of novel genetic ring oscillators. *eLife* **4**, e09771. (doi:10.7554/eLife.09771)
81. Hussain F, Gupta C, Hirning AJ, Ott W, Matthews KS, Josic K, Bennett MR. 2014 Engineered temperature compensation in a synthetic genetic clock. *Proc. Natl Acad. Sci. USA* **111**, 972–977. (doi:10.1073/pnas.1316298111)
82. Kim JK, Chen Y, Hirning AJ, Alnahhas RN, Josic K, Bennett MR. 2019 Long-range temporal coordination of gene expression in synthetic microbial consortia. *Nat. Chem. Biol.* **15**, 1102–1109. (doi:10.1038/s41589-019-0372-9)
83. Chen Y, Kim JK, Hirning AJ, Josic K, Bennett MR. 2015 Emergent genetic oscillations in a synthetic microbial consortium. *Science* **349**, 986–989. (doi:10.1126/science.aaa3794)
84. Prindle A, Samayoa P, Razinkov I, Danino T, Tsimring LS, Hasty J. 2012 A sensing array of radically coupled genetic 'biopixels'. *Nature* **481**, 39–44. (doi:10.1038/nature10722)
85. Danino T, Mondragon-Palomino O, Tsimring L, Hasty J. 2010 A synchronized quorum of genetic clocks. *Nature* **463**, 326–330. (doi:10.1038/nature08753)